AIAA JOURNAL
Vol. 33, No. 11, November 1995

Effect of Shock Strength on Oblique Shock-Wave/Vortex Interaction

Michael K. Smart* and Iraj M. Kalkhoran†
Polytechnic University, Brooklyn, New York 11201

An experimental study of the interaction between streamwise vortices and two-dimensional oblique shock waves has been conducted at Mach 2.5. The experiments involved positioning an instrumented two-dimensional wedge downstream of a semispan wing so that the trailing tip vortex from the wing interacted with the oblique shock wave formed over the wedge surface. The experiments were designed to simulate interaction of streamwise vortices with shock waves formed over aerodynamic surfaces or in supersonic inlets. The influence of oblique shock wave intensity on this inherently three-dimensional interaction was examined for vortices of variable strength. Results indicate that the interaction of a moderate strength vortex with an oblique shock wave can lead to the formation of a steady separated shock structure upstream of the oblique shock front. A significant expansion of the vortex core is observed in these cases, and the scale of the structure increases with shock wave intensity. In some instances the separated shock structure continues through the oblique shock front to strike the shock-generating wedge forming a three-dimensional shock-wave/boundary-layer interaction. The experiments indicate that significant distortion of streamwise vortices can be precipitated by oblique shock fronts with supersonic downstream conditions.

Nomenclature

d	= vortex core diameter
L	= length of wedge surface
M	= Mach number
P	= pressure
V	= velocity
x, y, z	= Cartesian coordinates
α	= vortex generator angle of attack
β	= shock angle
Γ	= circulation
θ	= flow deflection angle over wedge
μ	= Mach angle, $\sin^{-1}(M)$
ν	= uncertainty
ξ	= vorticity
ρ	= density

Subscripts

a	= axial
axis	= vortex axis
n	= normal
s	= swirl
T	= total
t	= tangential
w	= wedge
0	= chamber
1	= condition ahead of shock
2	= condition behind shock
∞	= freestream

Introduction

CONCENTRATED streamwise vortices occur in many aeronautical applications such as the flow past wings and slender bodies at angle of incidence. They are formed by the separation and subsequent roll-up of the thin viscous sheet near a surface that, once away from the surface, then convects downstream with the surrounding flow. This concentrated rotational region contained in a generally irrotational flow may then interact with other components of an aircraft or body of interest. For example, the vortices shed by the forebody or canards of a high-speed aircraft flying at angle of attack may pass over or strike its wings and aft control surfaces leading to loss of lift, increased drag, or changes in the pitching moment characteristics of the aircraft. Another deleterious possibility is the ingestion of streamwise vortices by the air intake systems resulting in decreased engine performance or blockage of the engine intake. The flowfields generated by such encounters are in general three dimensional and at supersonic speeds exhibit strong compressibility effects due to the presence of shock waves.

The strength of streamwise vortices steadily increases with the angle of incidence of the wing or body until a drastic disruption to its structure occurs, commonly called "vortex breakdown."[1-4] This phenomenon is characterized by a sudden increase in the size of the vortex, the appearance of reversed flow and a stagnation point on its axis, and the presence of large-scale unsteadiness. It is well known that in low-speed flows vortex breakdown may also be precipitated in a streamwise vortex by the application of a sufficiently strong adverse pressure gradient.[5] A considerable number of investigations have been reported in this area, including several review articles by Hall,[6] Liebovitch,[7] and most recently by Delery.[8] In supersonic flows it has been experimentally demonstrated that vortex breakdown can result from the interaction of sufficiently strong streamwise vortices with normal shock waves.[9-11] The interaction of vortices with shock waves and in particular supersonic vortex breakdown has been investigated by a few authors but has only recently attracted serious attention.

Shock-wave/vortex interactions are generally separated into two distinct classifications: normal shock-wave/vortex interactions (NSVI) and oblique shock-wave/vortex interactions (OSVI) (Fig. 1). Interaction of a vortex with a normal shock wave always results in a change from supersonic flow (a supercritical region incapable of admitting upstream wave propagation) to subsonic flow (a subcritical region that allows upstream propagating waves). The interaction of a vortex with an oblique shock wave does not necessarily involve a supercritical to subcritical transition, as the flow generally remains supersonic behind the shock wave. An examination of the shock-wave/vortex interaction problem indicates that the governing similarity parameters are the freestream Mach number M_∞, the freestream Reynolds number (with d as the characteristic length), a vortex intensity parameter such as $\Gamma/V_\infty d$, and the shock angle β. In addition to these parameters, it is important to note that the structure of the interaction will also depend upon the Mach number distribution of the incoming vortex.

Received June 17, 1994; presented as Paper 95-0098 at the AIAA 33rd Aerospace Sciences Meeting, Reno, NV, Jan. 9–12, 1995; revision received Feb. 3, 1995; accepted for publication Feb. 7, 1995.

*Graduate Research Fellow, Aerospace Engineering Department. Student Member AIAA.

†Assistant Professor, Aerospace Engineering Department. Member AIAA.

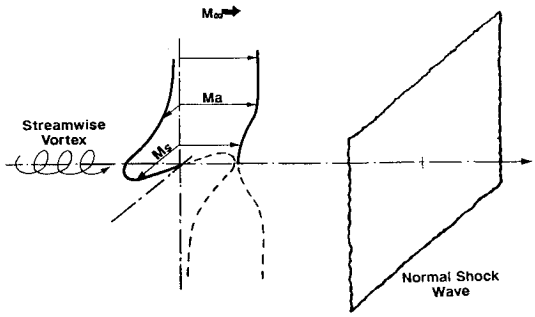

a) Normal shock-wave/vortex interaction

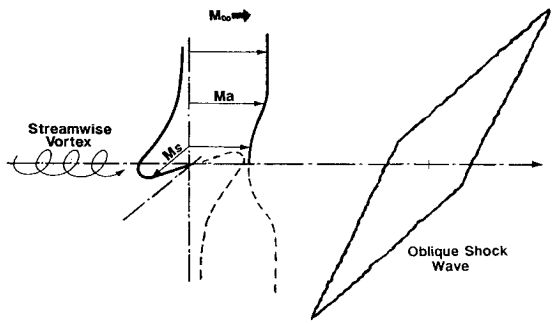

b) Oblique shock-wave/vortex interaction

Fig. 1 Shock-wave/vortex interaction classifications.

Introduction of a streamwise vortex upstream of an otherwise planar shock wave will in general lead to curvature of the shock front due to gradients of Mach number and total pressure in the vortex. Examining the geometry of the NSVI shown in Fig. 1a, if the shock wave remained normal to the freestream during the interaction, the vortex swirl would be at all times tangent to the shock wave and therefore have no effect upon it. However, as the shock wave deforms in response to axial Mach number and total pressure gradients in the vortex core, the swirl will contribute to the shock curvature in a nonuniform manner depending on the local component of swirl Mach number normal to the shock front. It is clear therefore that the interaction of a streamwise vortex with a normal shock wave will in general lead to a three-dimensional curvature of the shock front. For the special case of an axisymmetric streamwise vortex, the curved shock front will degenerate to an axisymmetric form. Examining the geometry of the OSVI shown in Fig. 1b, the fact that the undisturbed shock front is not normal to the freestream introduces an extra "nonsymmetric" element to the shock wave curvature produced by a given streamwise vortex. A three-dimensional curvature of the shock front will always occur in this case, even if the incoming vortex is axisymmetric. In summary, all shock-wave/vortex interactions include a three-dimensional curvature of the shock wave, which for the special case of the interaction between an axisymmetric streamwise vortex and a normal shock wave degenerates to an axisymmetric form.

A first step in the analysis of any shock-wave/vortex interaction is the determination of the three-dimensional curved shock front. Given that this nontrivial task has been accomplished, the changes in the vortex properties across the shock wave are of interest, in particular the change in its vorticity. Fundamental studies by Hays[12] demonstrated that the vorticity jump ($\delta\xi$) across a general three-dimensional steady curved shock is given by

$$\delta\xi_n = 0 \tag{1}$$

$$\delta\xi_t = \bar{n} \times [\nabla_t(\rho_1 V_{1n})/\delta\rho - \bar{V}_{1t} \cdot \nabla_t \bar{V}_{1t} \delta\rho/(\rho_1 V_{1n})] \tag{2}$$

In Eqs. 1 and 2 above, the subscripts n and t indicate components normal and tangential to the shock surface and $\bar{n}$ is its local unit normal. It is clear from these equations that there is no vorticity jump normal to the shock surface and that the vorticity jump tangent to the shock surface depends only on the density jump across the shock ($\delta\rho$) and the upstream properties. Because of the shock wave curvature inherent in all shock-wave/vortex interactions, a streamwise vortex will undergo a change in its vorticity for both NSVI and OSVI alike.

Previous experimental and numerical studies relevant to the interaction problem have concentrated on the interaction of streamwise vortices with normal shock waves. Delery et al.[9] carried out an experimental study of the interaction between streamwise vortices of nearly constant axial Mach number and normal shock waves, reporting some shock-induced modifications to both the structure and trajectory of the vortices. Their results indicated that interactions that precipitated vortex breakdown showed negative axial velocity at the vortex axis, a considerable reduction in maximum tangential velocity, and an increase in the radius of the vortex core. Based on these experiments they established a vortex breakdown limit as a function of vortex swirl rate and shock wave intensity. A companion numerical study was reported with the experiments[9] using the steady axisymmetric Euler equations and a prescribed Burgers' vortex with constant axial Mach number. A breakdown limit similar to the experiments was predicted, but the numerical simulation was not able to accurately calculate flow structure downstream of the breakdown.

Interaction of normal shock waves with vortices generated by a swirling vane injector was studied experimentally by Metwally et al.[10] and Cattafesta and Settles.[11] Cone probe measurements[10,11] showed that the vortices used in these experiments exhibited a wake-like axial Mach number in combination with a strong swirl. Both studies reported a strong influence of vortex swirl rate and Mach number on the interaction, a vortex breakdown, and an oscillating upstream shock propagation. Based on their experiments, Metwally et al.[10] suggested a hypothetical supersonic vortex breakdown model consisting of a region of reversed flow as well as a stagnation point downstream of a bulged-forward shock wave. The interaction of supersonic wing tip vortices with normal shock waves in an inlet type configuration was experimentally investigated by Zatoloka et al.[13] They reported development of a stagnation zone as a result of the encounter and also showed some distorted shock patterns. Experiments involving the head-on interaction of wing tip vortices with the leading edge of a shock-generating wedge were reported by Kalkhoran.[14] This interaction is different from the studies mentioned earlier as a stagnation point is forced to occur in the flow at the wedge leading edge. It was observed[14] that this encounter resulted in formation of an unsteady detached shock structure far upstream of the wedge leading edge and an expanded vortex core. It was not clear in these experiments[14] whether the detected unsteadiness was due to an observed unsteady tip vortex trajectory or whether it was a feature of the head-on interaction.

The aforementioned studies all involved interaction of streamwise vortices of different types with normal shock waves. Previous studies of the OSVI problem include numerical work by Corpening and Anderson,[15] in which the steady three-dimensional Euler equations were used to study interaction of constant axial Mach number vortices with oblique shock waves at Mach 2.28 and 5.0. They observed no vortex breakdown or appreciable alteration of vortex strength as a result of interactions but did report a deformation of the planar shock into a three-dimensional convex-concave shock shape. An experimental study of the interaction between wing tip vortices and oblique shock waves was reported by Kalkhoran and Sforza.[16] In this study a tip vortex from a rectangular half-wing encountered an oblique shock wave in close proximity to a 27-deg two-dimensional wedge at Mach 3. Vortex strength and separation distance between the vortex and the wedge leading edge were varied while the shock strength remained constant. An unsteady interaction was observed, and time-averaged wedge surface pressure measurements showed significant suction on the forward portions of the wedge. An unsteady tip vortex trajectory was observed in a similar fashion to Ref. 14. Rizzetta[17] conducted a numerical study of these experiments incorporating both the time-dependent three-dimensional Euler and mass-averaged Navier–Stokes equations. This study differed from previous numerical work on the interaction problem[9,15] in that the vortex generation was included in the numerical model. The results showed wedge surface pressure distributions similar to the experiments for some of the cases examined. However, in contrast to the experiments, no vortex distortion or unsteadiness was predicted.

The OSVI study reported here was conducted at Mach 2.5 with a similar experimental configuration to that used in Ref. 16. The experiments involved positioning an instrumented two-dimensional wedge downstream of a semispan wing so that the trailing tip vortex from the wing interacted with the oblique shock wave well above the wedge surface. The essential aim of the study was to examine the effect of shock strength on OSVI, a facet of the shock-wave/vortex interaction problem not previously addressed. Furthermore, the study was designed to investigate vortex distortion phenomenon during OSVI, in lieu of the fact that numerical solutions of the problem[15,17] have not indicated any vortex distortion or breakdown. Modifications to the experimental configuration of Ref. 16 include a simpler vortex generator wing geometry, a variable angle shock-generating wedge, and the installation of miniature high-frequency pressure transducers at the wedge surface. In addition, the study was conducted in a Mach 2.5 wind tunnel[18] of larger size than the Mach 3 facility used for the previous studies.[14,16]

Experimental Program

Wind Tunnel and Test Conditions

The current investigation was conducted in Polytechnic University's supersonic wind-tunnel facility.[18] It is an intermittent blowdown wind tunnel with a square test section of 381 mm × 381 mm and is capable of producing unit Reynolds numbers in the range of 26×10^6 to 22×10^7 per meter over a Mach number range from 1.75 to 4.0. The interaction studies reported here were conducted at a nominal test section Mach number of 2.49. The stagnation pressure and temperature for these experiments were 0.45 MPa and 290 K, respectively, resulting in a unit Reynolds number of 4.3×10^7 per meter. A typical test time for the experiments was 3 s.

Experimental Arrangement

An illustration of the experimental arrangement used for this study is shown in Fig. 2, followed by a dimensioned drawing in Fig. 3. The vortex generator was a rectangular half-wing with a diamond shaped cross section (8-deg half-angle), a chord length of 50.8 mm, a span of 165.1 mm, and angle-of-attack capability from 0 to 10 deg. The shock wave generator was a two-dimensional wedge section with an included angle of 20 deg, a wedge surface length of 76.2 mm, and a span of 177.8 mm. The wedge had variable angle-of-attack capability from 0 to 10 deg that enabled generation of flow deflections between 20 and 30 deg. The shock generator section was equipped with a 6 × 3 grid of equally spaced pressure ports in which miniature high-frequency pressure transducers were mounted. The six rows spanning the wedge were equally spaced between $x/L = 0.17$ and 0.75 (where x is the distance from the wedge leading edge). The three streamwise rows were located at $y/L = 0.12, 0.0$, and -0.12 (where $y = 0.0$ is directly behind the half-wing). The wedge was placed 152 mm (3 vortex generator chords) downstream of the half-wing trailing edge, with its leading edge 25 mm below the half-wing tip. The dimensions and relative orientation of the half-wing and the wedge section were chosen so that the interaction took place well above the wedge surface and within the "test diamond" of nearly uniform flow formed by the shock-expansion wave structure emanating from the half-wing.

Instrumentation, Data Acquisition, and Uncertainty Estimates

Miniature high-frequency pressure transducers (Kulite model XCQ-062-50A) with range of 0–345 kPa were used in the experiments. These had an outer diameter of 1.6 mm and a natural frequency response of 50 kHz. The amplified transducer outputs were digitized using a Metrabyte das-16, 12-bit analog-to-digital converter board at a rate of 500 Hz per channel. Shadowgraphs were taken of the flowfield at a rate of two per second using a spark light source that provided microsecond range exposure times. The errors associated with typical wedge and chamber pressure measurements reported in this work were $v_w = \pm 1.70$ kPa and $v_0 = \pm 2.72$ kPa, respectively. Based on these values, a typical uncertainty estimate for P_w/P_0 is listed in Table 1, along with typical uncertainty estimates for the axial Mach number and total pressure values extracted from Ref. 19.

Table 1 Uncertainty estimates

Property	Uncertainty estimate
P_w/P_0	± 0.0042
M_a	± 0.066
P_T/P_0	± 0.025

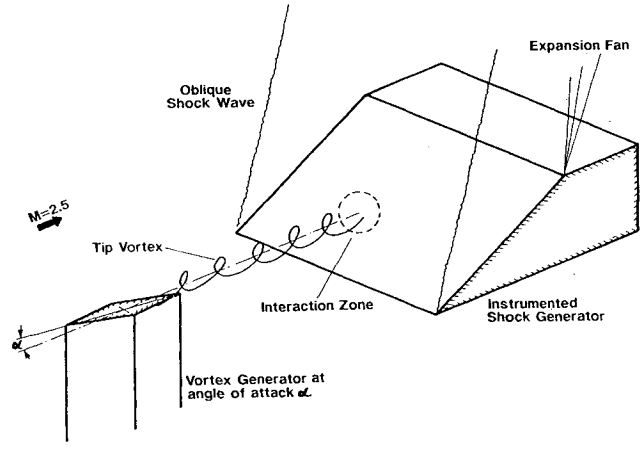

Fig. 2 Illustration of experimental arrangement.

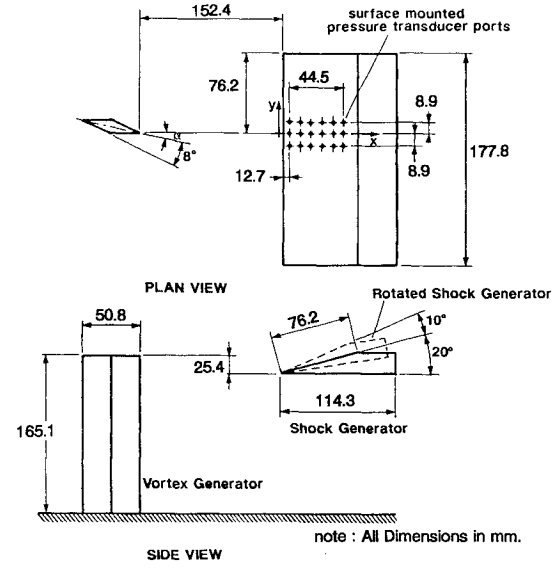

Fig. 3 Geometry of experimental arrangement.

Test Program

Experiments were carried out to systematically investigate the effect of shock wave strength on the interaction of wing tip vortices with two-dimensional oblique shock fronts. Tests were performed for the shock waves generated by flow deflections of $\theta = 22$, 25, and 29 deg. For each flow deflection angle a baseline run was conducted with the half-wing removed, followed by runs with the half-wing at $\alpha = 5$ and 10 deg. For each combination of θ and α, time-dependent pressure measurements were made at the 18 grid positions on the wedge, together with multiple spark shadowgraphs. Throughout the entire test program approximately 30% of the runs were repeated to check for consistency. It was found that the results were repeatable to well within the calculated accuracy of the instrumentation. For the purposes of this study, the tip vortex generated by the half-wing at $\alpha = 5$ deg will be referred to as the weak vortex, and interactions involving it will be called weak interactions. Correspondingly, the tip vortex generated by the half-wing at $\alpha = 10$ deg will be referred to as the strong vortex, and interactions involving it will be called strong interactions.

Experimental Results and Discussion

Wedge Calibration and Tip Vortex Characterization

Wedge calibration experiments were performed to establish the baseline pressure distribution on the wedge. The time-averaged streamwise pressure distributions for $\theta = 22$, 25, and 29 deg are shown in Fig. 4. These results compare favorably with two-dimensional theory, except for the downstream portion of the $\theta = 29$ deg case. The pressure relief observed in this case is a consequence of the fact that the shock-generating wedge does not span the entire width of the test section, giving rise to some three-dimensional effects at the edges. Figure 5 shows a typical shadowgraph of the baseline flowfield for the particular case of $\theta = 25$ deg. The oblique shock wave shown is close to the angle predicted by two-dimensional theory ($\beta = 50.4$ deg). The disturbances appearing in the shadowgraph downstream of the oblique shock are generated at the wedge supports and are far removed from the interaction zone.

Conical probe measurements of the supersonic wing tip vortices generated for the current work were reported in Ref. 19. These measurements[19] consisted of vertical (spanwise with respect to the half-wing) surveys through the axes of the wing tip vortices at a distance 2.25 chords downstream of the half-wing trailing edge. As indicated in Figs. 6 and 7, which have been extracted from Ref. 19, the wing tip vortices are regions of total pressure deficit and wake-like axial Mach number. The magnitude of these deficits in total pressure and axial Mach number increase with angle of attack of the half-wing. The conical probe measurements[19] also showed an asymmetric "Burgerlike" swirl distribution in the wing tip vortices and vortex core diameters of 4.0 and 5.5 mm for the weak and strong vortices, respectively. Spark shadowgraphs of the vortices indicated no change of the vortex trajectories with time, in contrast to the unsteady inwash observed in Refs. 14 and 16. No influence of the shock-expansion wave structure generated by the half-wing was observed.[19]

Weak Interaction Results

Figure 8 illustrates a typical shadowgraph of the flowfield resulting from the interaction of the weak vortex with a two-dimensional oblique shock wave, i.e., a weak interaction. The particular case

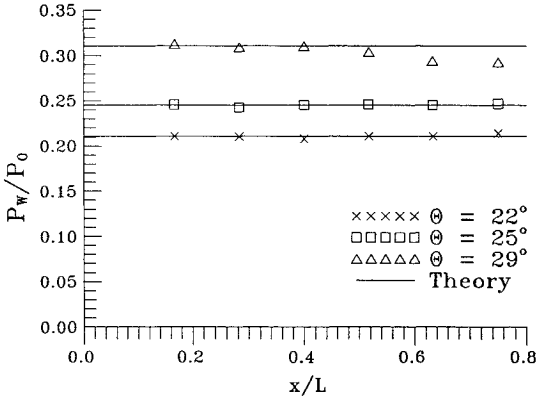

Fig. 4 Baseline wedge pressure distributions.

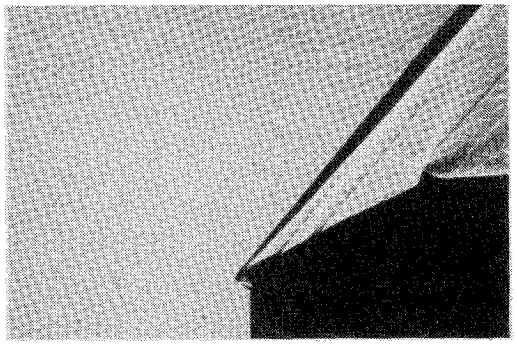

Fig. 5 Shadowgraph of baseline flowfield with $\theta = 25$ deg.

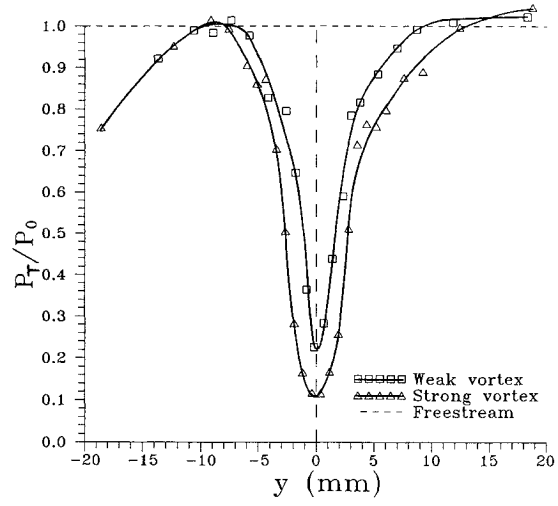

Fig. 6 Total pressure distributions in the wing tip vortices.

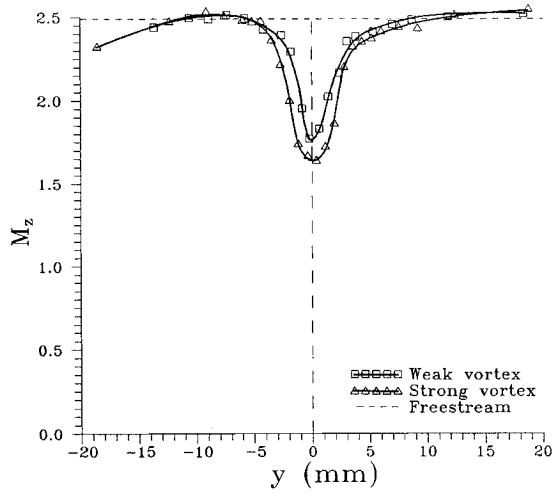

Fig. 7 Axial Mach number distributions in the wing tip vortices.

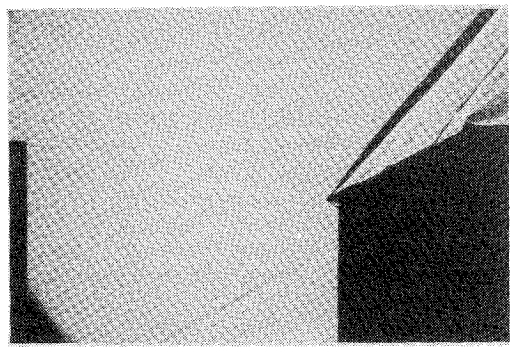

Fig. 8 Shadowgraph of the weak interaction flowfield with $\theta = 25$ deg.

shown in Fig. 8 involves the shock wave generated by $\theta = 25$ deg. Flow is from left to right with the half-wing in the lower left-hand corner and the wedge section on the right. The shadowgraph clearly indicates a concentrated tip vortex convecting downstream and intersecting with the oblique shock wave well above the wedge surface. A comparison with Fig. 5 indicates that the presence of the weak vortex has moved the shock wave slightly upstream of its undisturbed position, a movement consistent with a wakelike axial Mach number in the vortex. Downstream of the shock wave the vortex appears to be convected with the mainstream, although the view is obscured by waves from the wedge edge effects. This flow structure is typical of the weak interactions observed in this study. Variation of the shock wave intensity did not produce any substantial changes to

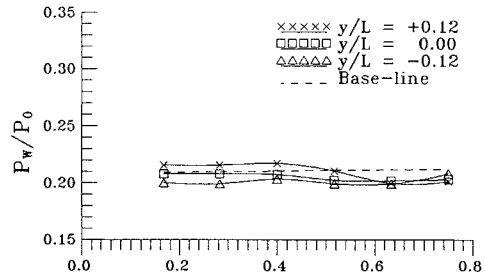

a) θ = 22 deg

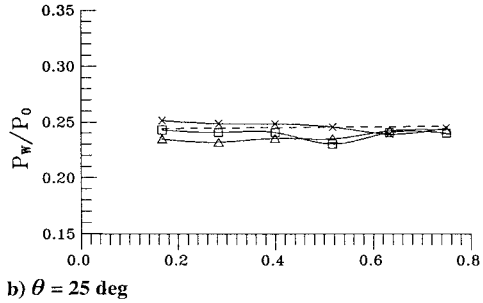

b) θ = 25 deg

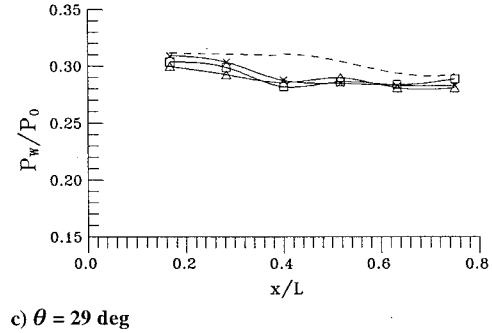

c) θ = 29 deg

Fig. 9 Time-averaged wedge pressure distributions for the weak interactions.

the flow structure, and multiple shadowgraphs taken during typical 3-s runs showed no changes with time.

Time-averaged wedge surface pressure distributions for the weak interactions are shown in Figs. 9a–9c for $\theta = 22$, 25, and 29 deg, respectively. The dashed lines in the figures correspond to the baseline data, and the solid lines represent the streamwise pressure distributions at $y/L = 0.12$, 0.0, and -0.12. Examination of Fig. 9b ($\theta = 25$ deg) indicates that the streamwise variation of pressure is similar at each position. At $y/L = 0.0$, for example, the pressure is constant up to approximately $x/L = 0.4$, followed by a suction that reaches a minimum at $x/L = 0.52$ and finally a return towards the baseline pressure at $x/L = 0.63$. Pressures at $y/L = 0.12$ are the highest, $y/L = -0.12$ are the lowest, and pressures at $y/L = 0.0$ are in between. This description of the pressure distribution in Fig. 9b is also applicable to Figs. 9a and 9c ($\theta = 22$ and 29 deg), except that the disruption to constant pressure begins at $x/L = 0.5$ and 0.25, respectively. The localized wedge suction is of similar magnitude (approximately 7% of baseline) and similar streamwise scale for all three shock strengths. It is noted that the pressure measurements showed no large-amplitude fluctuations during typical 3-s test periods.

The time-averaged pressure measurements show some interesting features of the OSVI. The spanwise pressure variation on the wedge is believed to be due to the fact that the component of velocity normal to the oblique shock is not uniform in the vortex. In the present geometry, the vortex swirl velocity adds to the normal velocity component for positive y and subtracts from the normal velocity component for negative y. This leads to a locally stronger shock for positive y (creating a higher pressure on the wedge) and a locally weaker shock for negative y (creating a lower pressure on the wedge). Superimposed on this is the fact that there is a pressure deficit in the vortex with respect to the freestream, and hence the wedge pressure at $y/L = 0.0$ is also lower than the baseline value.

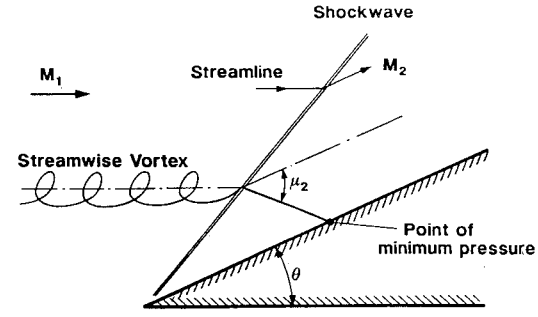

Fig. 10 Wave diagram for flow downstream of the weak interaction.

The localized wedge suction observed for all three shock strengths is thought to be due to waves emanating from the interaction zone. The incoming wing tip vortex consists of a region of total pressure and axial Mach number deficit, combined with a swirl. As the shock distorts due to passage of the vortex, waves are generated in the supersonic flow behind the shock that propagate towards the wedge. It is postulated that these waves are the cause of the low-pressure region and therefore must be expansion waves. Evidence to support this postulation can be obtained by calculating the point at which waves from the interaction zone would be expected to reach the wedge. A simple first-order estimate of the expected point of minimum pressure can be obtained by assuming that shock distortion and variations in μ behind the shock are small. Using the geometry shown in Fig. 10, the wave emanating from the point of intersection of the vortex axis and the oblique shock wave reaches the wedge at $x/L = 0.64$, 0.59, and 0.45 for $\theta = 22$, 25, and 29 deg, respectively. These values correspond reasonably well with the observed positions of minimum pressure in each case.

In summary, the weak interaction tests showed slight distortion of the oblique shock wave for all three shock strengths. Spanwise variation in the wedge pressure was observed to occur due to vortex swirl, together with a localized wedge suction. The streamwise position of the localized wedge suction moved forward with increased shock wave intensity, whereas its magnitude and streamwise scale remained unchanged.

Strong Interaction Results

The strong interaction results exhibit many characteristics similar to the weak interactions; however, the increased vortex strength causes some dramatic changes in the flowfield to occur. Figures 11a–11c show spark shadowgraphs of the strong interaction for $\theta = 22$, 25, and 29 deg, respectively. The strong tip vortex can be seen in each of the shadowgraphs to convect smoothly downstream and enter an OSVI well above the shock-generating wedge. Examination of Fig. 11c indicates that for $\theta = 29$ deg, the strong interaction precipitates a dramatic change in the structure of the shock wave and a considerable disruption to the vortex. For this case the shadowgraph depicts the formation of a local three-dimensional shock structure well upstream of the undisturbed oblique shock wave, which surrounds an expanding vortex core in much the same manner as a shock wave forms about a blunted body. It appears that the Mach number and total pressure deficits associated with the strong vortex are of such a magnitude that an oblique or slightly deformed shock wave cannot be sustained in the interaction zone. The original shock wave breaks down in this region, and the flow responds by changing to a different structure that includes an upstream shock propagation. In a sense, the shock wave locally separates from the surrounding shock to form an independent structure. The term "separated shock structure" will be used to describe this phenomenon in the current work.

Multiple spark shadowgraphs taken during typical 3-s runs show no change in the scale or shape of the separated shock structure with time. Hence it appears that the conditions that force the shock wave to separate locally are equilibrated by the formation of this structure. The separated shock wave is normal to the freestream

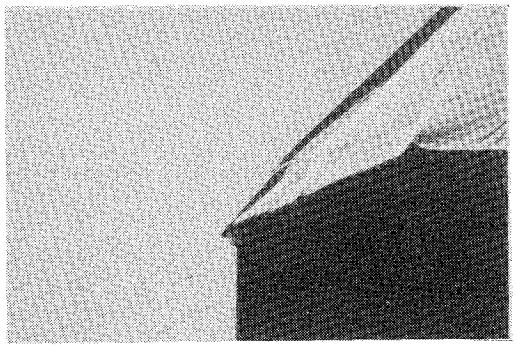

a) $\theta = 22$ deg

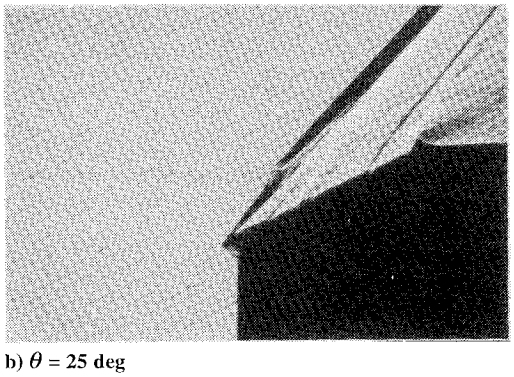

b) $\theta = 25$ deg

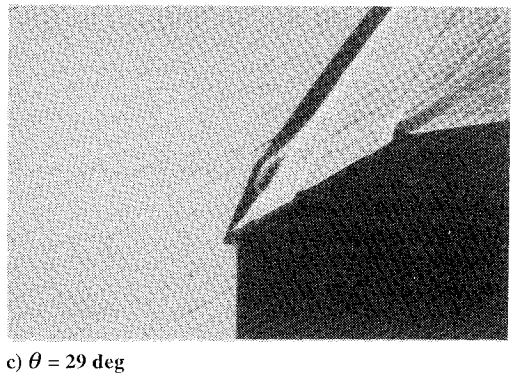

c) $\theta = 29$ deg

Fig. 11 Shadowgraphs of the strong interaction flowfields.

at the vortex axis, locally forming a NSVI and therefore a local subsonic region downstream of the shock. After passing through this normal shock wave, the vortex core is seen to expand considerably. Away from the vortex axis the observed separated shock structure appears to be simply a response of the surrounding mainstream to the expansion of the vortex core. This shock structure is similar to that reported for the head-on interaction of a wing tip vortex with a wedge leading edge reported in Ref. 14, except for the fact that the head-on interaction was found to be unsteady. The fundamental difference between the head-on vortex/wedge interaction[14] and the current work is the presence of a forced stagnation point in the interaction zone of the head-on encounter.[14] This difference may be the reason for the observed unsteadiness reported in Ref. 14.

Characteristic features of incompressible vortex breakdown are the appearance of reversed flow and a stagnation point, a sudden increase in the size of the vortex, and the presence of large-scale unsteadiness. Despite the fact that the existence of reversed flow and a stagnation point cannot be verified in this study, Fig. 11c indicates a strong visual resemblance to the low-speed vortex breakdown reported in the literature.[1-3] Even though a categorical statement that Fig. 11c depicts a form of vortex breakdown cannot be made in this case, these observations clearly demonstrate that severe distortion of a vortex can occur during OSVI, in contrast to the two numerical studies of the problem.[15,17] Corpening and Anderson[15] suggested that the absence of breakdown in their numerical studies of OSVI may be due to the presence of supersonic flow downstream of the oblique shock wave, i.e., a supersonic downstream boundary condition. The current observations indicate that a supersonic downstream condition does not necessarily prohibit severe vortex distortion or possibly even vortex breakdown.

Another interesting feature of the strong interaction shown in Fig. 11b ($\theta = 25$ deg), and to the authors' knowledge not previously reported, is the continuation of the separated shock through the plane of the undisturbed oblique shock wave to impinge on the wedge surface. The lower portion of the shock is clearly seen to strike the wedge at approximately $x/L = 0.3$ in this case and forms a three-dimensional shock-wave/boundary-layer interaction on the wedge surface. The details of the region where the lower portion of the separated shock structure crosses the original oblique shock wave is obscured in the shadowgraph, but the two appear to interact as independent shock waves of different families, with the local downstream angle of both dictated by the need to match flow angle and static pressure.

The effect of shock wave intensity on the strong interaction is clearly shown by comparing Figs. 11a–11c. In Fig. 11a ($\theta = 22$ deg) the separated shock structure appears to be just on the verge of formation. The oblique shock wave shows significant deformation in the interaction region, but no separate structure can be clearly seen. In Fig. 11b ($\theta = 25$ deg) the separated shock structure is fully formed with the leading portion located 6.7 mm upstream of the undisturbed oblique shock wave. Finally, Fig. 11c ($\theta = 29$ deg) shows a separated shock wave with the leading portion located 13 mm upstream of the undisturbed oblique shock, the largest of the three cases examined. It appears that the effect of increased oblique shock wave intensity on the strong interaction is an increase in the scale of separated shock structure. The position at which the lower portion of the separated shock impinges on the wedge surface also varies with the shock wave intensity. For $\theta = 22$ deg no shock wave was observed to impinge on the wedge surface. As already stated, the $\theta = 25$ deg case leads the lower portion of the separated shock to strike the wedge surface at $x/L = 0.3$. Increase of the flow deflection to $\theta = 29$ deg removes the impinging shock wave. This is thought to be because no downstream solution that includes a continuation of the separated shock wave through the oblique shock is possible for the $\theta = 29$ deg case. In general, it may be stated that the overall structure of the strong interaction is quite sensitive to the strength of the original oblique shock wave.

Time-averaged surface pressure distributions for the strong interactions are shown in Figs. 12a–12c for $\theta = 22$, 25, and 29 deg respectively. As for the weak interactions, the pressure measurements showed no large-amplitude fluctuations in typical 3-s test periods. Examination of Fig. 12b ($\theta = 25$ deg) indicates that some features of the pressure distribution are similar to the weak interaction. The vortex swirl leads to spanwise pressure variation once again, but with a greater magnitude due to the increased vortex strength. The streamwise pressure distributions at each spanwise position are similar once again but include a feature not apparent in the weak interactions. Figure 12b shows constant pressure up to $x/L = 0.25$, followed by a significant peak at $x/L = 0.4$, a substantial drop to a minimum at $x/L = 0.55$, and finally a return towards the baseline pressure at $x/L = 0.8$. The peak experienced at all spanwise locations at $x/L = 0.4$ was not observed for the weak interactions and appears to be in response to the separated shock wave shown in Fig. 11b to impinge on the wedge at approximately $x/L = 0.3$. The full pressure rise across the impinging shock may not be shown in these results due to the coarseness of the pressure port grid on the wedge. Downstream of the peak a significant suction is experienced on the wedge in a similar fashion to the weak interaction, but of considerably larger magnitude. The minimum pressure measured on the wedge for $\theta = 25$ deg is approximately 24% below the baseline.

Variation of shock wave intensity has a twofold effect on the wedge surface pressure for the strong interaction. Comparison of Figs. 12a–12c indicates that increasing shock strength moves the disrupted region (peak, trough, and return towards baseline) upstream and increases the relative magnitudes (compared with the baseline) of the wedge suction. The local pressure peak, however, is most prominent for $\theta = 25$ deg. The magnitude of the maximum suction for $\theta = 22$, 25, and 29 deg is 10, 24, and 31% of the respective baseline pressure. The scale of the disrupted region

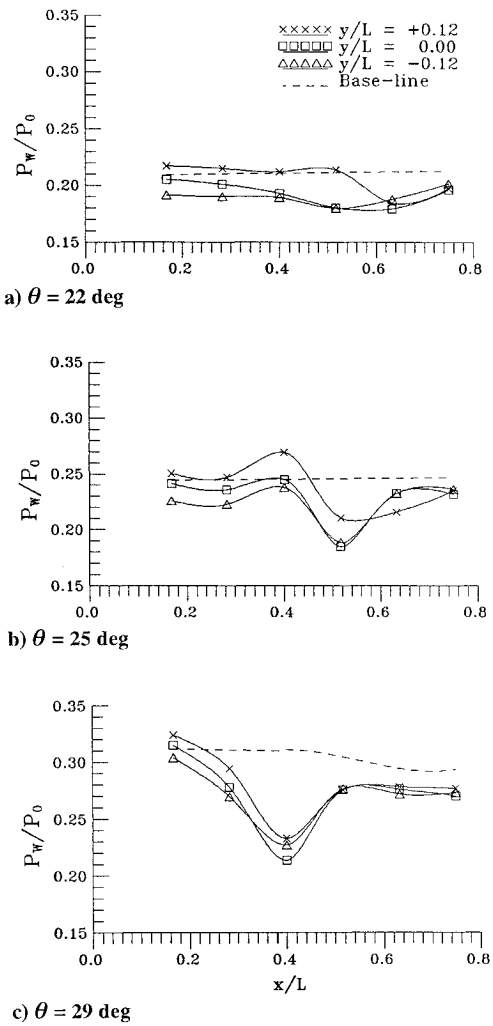

Fig. 12 Time-averaged wedge pressure distributions for the strong interactions.

does not vary with shock wave strength but is greater for the strong interaction than for the weak encounter. It is expected that the suction observed at the wedge is generated by waves emanating from the interaction zone in a similar fashion to the weak interaction. However, the presence of the separated shock structure in the strong interaction makes analysis of the expected wedge pressure far more difficult than for the weak interaction.

In summary, the strong interaction precipitated a local disruption of the oblique shock wave that took the form of a steady three-dimensional separated shock structure upstream of the undisturbed oblique shock front. This was accompanied by a significant expansion of the vortex core and a local subsonic region downstream of the separated shock. The scale and standoff distance of the structure increased with oblique shock wave intensity, and a portion of the separated shock was observed to impinge on the wedge surface for some oblique shock wave strengths. The pressure distributions on the wedge exhibited a similar form to the corresponding weak interaction results, except for a local pressure peak in the vicinity of shock wave impingement. The magnitude of the observed wedge suction was significantly larger than for the corresponding weak interaction.

Conclusions

The effect of shock wave strength on the interaction between wing tip vortices and oblique shock waves has been investigated at Mach 2.5. For the weak interaction, involving a vortex generated by the half-wing at $\alpha = 5$ deg, the oblique shock wave was slightly distorted for the three shock strengths investigated and the vortex appeared to be convected with the mainstream after the shock. Small changes from the baseline surface pressure were experienced on the shock-generating wedge. For the strong interaction, involving a vortex generated by the half-wing at $\alpha = 10$ deg, a local disruption of the oblique shock wave was observed in the interaction zone, which took the form of a steady separated shock structure upstream of the original oblique shock wave. This structure was accompanied by a significant expansion of the vortex core and a local subsonic region downstream of the separated shock. The upstream standoff distance and the scale of this structure increased with shock wave intensity. For some shock wave strengths a portion of the separated shock structure continued through the original oblique shock wave to strike the wedge and form a three-dimensional shock-wave/boundary-layer interaction. Significant changes from the baseline pressure were experienced on the wedge, including a localized suction at the midchord region of the wedge of up to 31% of the baseline pressure. The magnitude of the surface pressure variations and their position on the wedge varied with shock wave strength. It was observed in these experiments that severe distortion of supersonic streamwise vortices is not limited to normal shock waves, but can be precipitated by oblique shock fronts with supersonic downstream conditions. This exploratory study gives some insight into the nature of oblique shock-wave/vortex interaction and brings to light some interesting features of the problem that will require further study.

Acknowledgments

This work was supported by the Air Force Office of Scientific Research under Grant F49620-93-1-0009 and by NASA Lewis Research Center under Grant NAG3-1378. The assistance of Lester Orlick and Frank Wang was greatly appreciated during the work.

References

[1]Werle, H., "Sur l'eclatement des tourbillons d'apex d'une aile delta aux faibles vitesses," *La Recherche Aeronautique*, No. 74, Jan.–Feb. 1960, pp. 23–30.

[2]Lambourne, N. C., and Bryer, D. W., "The Bursting of Leading-Edge Vortices—Some Observations and Discussion of the Phenomenon," Aeronautical Research Council, Rept. 3282, London, April 1961.

[3]Harvey, J. K., "Some Observations of Vortex Breakdown Phenomenon," *Journal of Fluid Mechanics*, Vol. 14, 1962, pp. 585–592.

[4]Benjamin, T. B., "Theory of the Vortex Breakdown Phenomenon," *Journal of Fluid Mechanics*, Vol. 14, 1962, pp. 593–629.

[5]Sarpaka, T., "The Effect of Adverse Pressure Gradient on Vortex Breakdown," *AIAA Journal*, Vol. 12, No. 5, 1974, pp. 602–607.

[6]Hall, M. G., "Vortex Breakdown," *Annual Review of Fluid Mechanics*, Vol. 4, 1972, pp. 195–218.

[7]Leibovich, S., "Vortex Stability and Breakdown: Survey and Extension," *AIAA Journal*, Vol. 22, No. 9, 1983, pp. 1192–1206.

[8]Delery, J. M., "Aspects of Vortex Breakdown," *Progress in Aerospace Sciences*, Vol. 30, No. 1, 1994, pp. 1–59.

[9]Delery, J., Horowitz, E., Leuchter, O., and Solignac, J. L., "Fundamental Studies on Vortex Flows," *La Recherche Aerospatiale* (English ed.) (ISSN 0379-380X), No. 2, 1984.

[10]Metwally, O., Settles, G., and Horstman, C., "An Experimental Study of Shock Wave/Vortex Interaction," AIAA Paper 89-0082, Jan. 1989.

[11]Cattafesta, L. N., and Settles, G. S., "Experiments on Shock/Vortex Interaction," AIAA Paper 92-0315, Jan. 1992.

[12]Hayes, W. D., "The Vorticity Jump Across a Gasdynamic Discontinuity," *Journal of Fluid Mechanics*, Vol. 2, 1957, pp. 595–600.

[13]Zatoloka, V., Ivanyushkin, A. K., and Nikolayev, A. V., "Interference of Vortexes with Shocks in Airscoops. Dissipation of Vortexes," *Fluid Mechanics, Soviet Research*, Vol. 7, No. 4, 1978, pp. 153–158.

[14]Kalkhoran, I. M., "Vortex Distortion During Vortex-Surface Interaction in a Mach 3 Stream," *AIAA Journal*, Vol. 32, No. 1, 1994, pp. 123–129.

[15]Corpening, G., and Anderson, J., "Numerical Solutions to Three-Dimensional Shock Wave/Vortex Interaction at Hypersonic Speeds," AIAA Paper 89-0674, Jan. 1989.

[16]Kalkhoran, I. M., and Sforza, P. M., "Airfoil Pressure Measurements During Oblique Shock Wave-Vortex Interaction in a Mach 3 Stream," *AIAA Journal*, Vol. 32, No. 4, 1994, pp. 783–788.

[17]Rizzetta, D. P., "Numerical Simulation of Oblique Shock-Wave/Vortex Interaction," AIAA Paper 94-2304, June 1994.

[18]Kalkhoran, I. M., Cresci, R. J., and Sforza, P. M., "Development of Polytechnic University's Supersonic Wind Tunnel Facility," AIAA Paper 93-0798, Jan. 1993.

[19]Smart, M. K., Kalkhoran, I. M., and Bentson, J., "Measurements of Supersonic Wing Tip Vortices," *AIAA Journal* (to be published) (AIAA Paper 94-2576, June 1994).